Straw Bale Wall Hot Box Test Results and Analysis

Jeffrey E. Christian
Member ASHRAE

André O. Desjarlais

Therese K. Stovall, P.E.
Member ASHRAE

ABSTRACT

This paper documents the first known hot box test of a straw bale wall. The results led the authors on an investigative search for analytical solutions that accurately predicted the heat transfer occurring under steady-state hot box tests. The measured steady-state R-value of this two-tie wheat-straw bale wall does not agree with frequently assumed R-values for straw bale walls, based on limited individual bale thermal resistivity measurements. The hot box measurement area for this test wall was 2.4 m by 2.4 m (8 ft by 8 ft). Frequently reported R-values of straw bale walls are between 7 and 10.5 $m^2 \cdot °C/W$ (40-60 $h \cdot ft^2 \cdot °F/Btu$). The measured steady-state R-value for the straw bale wall, built according to the Tucson, Arizona, structural code, was 2.8 $m^2 \cdot C/W$ (16 $h \cdot ft^2 \cdot °F/Btu$). Total thickness of the complete wall was about 51 cm (20 in.). Test wall layers consist of 47 cm (18 in) thick bales stacked with the straws oriented perpendicular to the wall surfaces, the outside surfaced with stucco containing chicken wire lath, and the inside surfaced with two layers of 1.3 cm (½ in.) thick gypsum drywall mechanically fastened to 5 cm × 10 cm (2 in.× 4 in.) stakes pounded into the straw bales on 61 cm (2 ft) centers.

Thermal conductivity and air permeability measurements of the straw material are reported, with the straw oriented both parallel and perpendicular to the direction of air and heat flow. Several analytical models using the laboratory straw material property measurements as input are employed to generate analytical predictions for comparison with the hot box results. Natural convection within the wall was the major cause for the surprisingly low R-value hot box measurement. The convective loop formed within the wall follows a path starting with air rising between the straw bales and the drywall on the warm side, through the straws in the top row of bales, falling on the cold side between the straw and the stucco, through the bottom straws, and back to the air gap between the straw and the drywall on the warm side. A computational fluid dynamics model helped uncover that the natural convection does not occur predominately through the straw itself. The natural convection can occur within the gaps between the straw and the surface treatments on both the interior and exterior sides. The authors conclude that with careful application of interior plaster and exterior stucco, straw bale wall builders can build "natural convection free." Follow-up tests confirm that the major impacts of natural convection can be eliminated, which results in an R-value about 60% higher then the first wall reported in this paper.

INTRODUCTION

With the development of steam baling machinery, straw bales have been used as an inexpensive and abundant construction material in the United States since the 1880s, reaching a height of popularity between the years of 1915 and 1930. Since 1973 the high costs of conventional construction materials, concerns for improving environmental quality, and the trend toward using natural resources in a sustainable, environmentally responsible manner have contributed to a revival of interest in straw-bale construction (MacDonald and Myhrman 1995).

A major potential benefit of straw-bale exterior wall construction is very high thermal resistance to unwanted heat loss in the winter and heat gain in the summer. Independent research and anecdotal accounts using single bales of straw and a "modified guarded hot plate apparatus" have resulted in reports of straw bales having a thermal resistance of 7.6 $(m^2 \cdot °C)/W$ (R-value of 43 $(h \cdot ft^2 \cdot °F)/Btu$) with the heat

Jeffrey E. Christian is director of the Buildings Technology Center, **André O. Desjarlais** is a program manager, and **Therese K. Stovall** is a development engineer at Oak Ridge National Laboratory, Oak Ridge, Tenn.

flow parallel to the predominant orientation of the individual straws. This was measured on an 11 cm (4.5 in.) thick layer within a single bale and reported at a width of 47 cm (18 in.) (McCabe 1993). The average temperature of the 11 cm (4.5 in.) thick straw layer within the tested bale during measurement is reported to be 41.6°C (107°F).

As of July 1996, no ASTM C-236 guarded hot box test of a full-size straw bale wall was reported in the published literature nor on the Internet. With an increasing interest in sustainable construction techniques, a well-controlled investigation of the R-value of an entire straw-bale wall system, complete with a weather-resistant outer surface and esthetically suitable inner surface treatment, was requested by the Department of Energy's Office of Building Technology. In July 1996, 24 science teachers participating in the Appalachian Regional Commission Teacher Leadership Program built a straw bale wall in a test frame at Oak Ridge National Laboratory. The wall was instrumented and tested in ORNL's rotatable guarded hot box.

Literature Review Reveals Documented Test Results of Straw Bales as Insulation Material

The research project of McCabe (1993) on the thermal resistivity of straw bales for construction obtained R-values through a modified guarded hot plate procedure. The resistivity reported for a wheat straw bale with heat flow parallel to the grain was 16.5 m·°C/W (2.38 (h·ft^2·°F)/Btu·in.) or an R-value of 7.6 m^2·°C/W (43 (h·ft^2·°F)/Btu) for a width of 47 cm (18 in.) (McCabe 1993).

An innovative straw bale/mortar wall system built and tested through the Housing Technology Incentives Program of Canada Mortgage and Housing Corporation in Ottawa, Ontario, Canada, reported results of a resistivity of 13.1 m·°C/W (1.89 h·ft^2·°F/Btu·in.) or an R-value of 6.2 m^2·°C/W (35 h·ft^2·°F/Btu) for the 47 cm (18.5 in.) thick wall. The procedure for this testing was not available; however, it did have cement-lime-sand mortar on both sides of the wall (CMHC 1984).

A 1994 test by Sandia National Laboratories in Albuquerque, New Mexico, using a thermal probe in the center of a straw bale, resulted in an average resistivity of 18.6 m·°C/W (2.67 h·ft^2·°F/Btu·in.) or an R-value of 8.4 m^2·°C/W (48 h·ft^2·°F/Btu) for 46 cm (18 in.) bales. The thermal probe is a radial measurement of thermal conductivity; therefore, it measures a combination of heat flow at various angles to the straw fibers.

At Lawrence Berkeley National Laboratory, Huang (1995) ran DOE-2 simulations of straw bale houses proposed for the Navajo Nation in Arizona. The R-value assumptions used were approximately 10.6 m^2·°C/W (60 (h·ft^2·°F)/Btu).

None of the above procedures matched the Oak Ridge project, which included a full-scale wall tested in the ASTM C 236 guarded hot box. As evidenced by the impressive number of Internet sites devoted to the topic of straw bale construction, the enthusiasts come from a wide variety of backgrounds, including governmental agencies, universities, professional organizations, environmental groups, and the general public.

PROCEDURE

After reviewing how straw bales were being used to construct homes, it was decided that a 2.44 m × 2.44 m (8 ft × 8 ft) load-bearing wall, constructed to the Tucson, Arizona, structural code, would be built of straw bales with stucco on the exterior side and two layers of 1.3 cm (½ in.)gypsum board on the interior. The bales were each labeled, and the dimensions, density, and moisture content measured and recorded as shown in Table 1. Because straw bales are not uniformly shaped or sized, it was necessary to determine dimensional and structural similarity. An effective bale length of 0.945 m (3.1 ft) was established by determining the mean of ten bales. Twenty-one of the most similar straw bales were chosen, and half bales were created from three to facilitate the construction (see Figure 1).

Several special tools were made to construct the wall. A bale needle made of 0.6 cm (¼ in.) metal rod pounded flat, ground to a point at one end, and drilled with two holes for eyes was made according to the methods of MacDonald and Myhrman (1995). This was used to halve the three bales. Staples were constructed by bending six 1 m length reinforcement rods (see Figure 2). These were used to secure the half bales.

Figure 1 *Making half bales.*

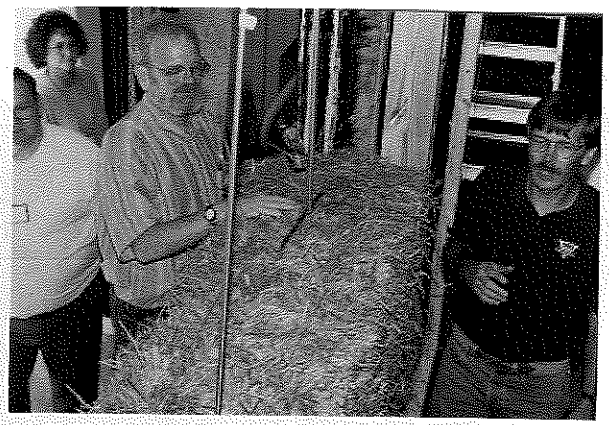

Figure 2 *Bale staples and compression rods.*

TABLE 1
Material Property Data for the Straw Bales[1]

Bale #	Dimensions			Volume	Mass	Density	Moisture
	L(cm)	W(cm)	H(cm)	(m^3)	(kg)	(kg/m^3)	Original % by Weight
1	97.8	47.0	35.6	0.163	13.6	83.1	11
2	90.2	43.9	35.6	0.141	13.0	92.6	<10
3[2]	94.0	48.3	35.6	0.161	13.4	83.1	10.5
4	94.0	48.3	35.6	0.161	13.8	85.4	11
5	90.2	48.3	35.6	0.155	12.8	82.5	10
6	94.0	48.3	35.6	0.161	13.2	81.7	<10
7	96.5	49.5	35.6	0.170	13.7	80.5	10
8	88.9	48.3	35.6	0.153	13.4	87.9	<10
9	91.4	47.0	35.6	0.153	13.7	89.8	12
10	95.3	48.3	35.6	0.163	13.4	81.7	11
11	94.0	45.7	35.6	0.153	14.0	91.6	11
12	88.9	45.7	35.6	0.145	12.0	83.0	10
13	97.8	48.3	35.6	0.168	11.9	70.7	<10
14	88.9	47.0	35.6	0.149	13.7	92.1	10
15	95.3	45.7	35.6	0.155	10.5	67.9	11
16	92.7	47.0	35.6	0.155	13.8	89.2	11
17	92.7	47.0	35.6	0.155	12.1	78.4	12
18	95.3	48.3	35.6	0.163	12.5	76.5	<10
19[2]	91.4	47.0	35.6	0.153	13.6	89.2	10
20	88.9	47.0	35.6	0.149	12.5	84.1	11
21	94.0	49.5	35.6	0.166	12.4	74.7	12
22[2]	92.7	48.3	35.6	0.159	13.3	83.4	11
23	94.0	49.5	35.6	0.166	14.6	88.4	11
24	91.4	47.0	35.6	0.153	11.2	73.2	13
25	97.8	47.0	35.6	0.163	12.8	78.4	12
26	90.2	47.0	35.6	0.151	13.9	92.6	12
27	92.7	48.3	35.6	0.159	12.7	79.7	12
28	94.0	48.3	35.6	0.161	14.2	87.9	11
29	92.7	47.0	35.6	0.155	14.6	94.4	11
30	92.7	48.3	35.6	0.159	15.9	99.9	20.5
Average	93.0	47.5	35.6	0.157	13.2	84.1	

[1] To convert to inch-pound units, multiply cm by 0.39 to obtain in., m^3 by 35.3 to obtain ft^3, kg/m^3 by 0.0624 to obtain lb/ft^3.
[2] Data refer to full original length bales.

Figure 3 *Splash barrier and termite screen were installed.*

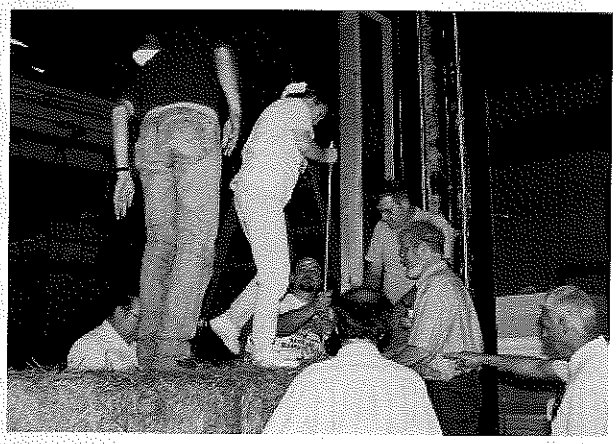

Figure 4 *Compression rods help compress the wall.*

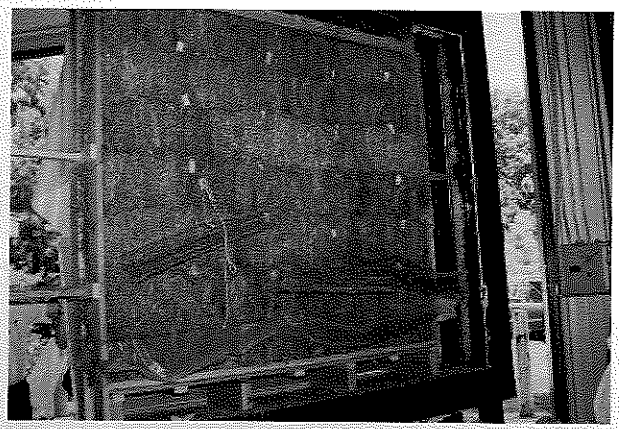

Figure 5 *Wood stakes pounded into the straw are used to fasten the drywall.*

Aluminum flashing was cut for use as a termite barrier under the bottom row of three bales. Plastic film was cut for use as a moisture barrier over the bottom row of three bales (see Figure 3). Three compression rods for compacting the straw bales were made from all-thread 1.3 cm (½ in.) steel rods by connecting two 4 ft lengths (see Figure 4). Twenty-four wood stakes were made from 2 × 4s, cut into 2 ft lengths and sharpened. They were used as studs for mounting the gypsum board. The ends of these stakes can be seen in the wall prior to installation of the gypsum in Figure 5.

Next, the structural framework was designed and constructed as shown in Figure 6. A knee wall was used to support seven layers of bales in the 2.4 m (8 ft) high wall. The knee wall also served to provide access to the three compression rods. Two 2 in. × 6 in. wood framing members served as side braces on each side and extended above the top plate. The top plate was constructed of 2 in. × 6 in. wood framing members on each side, which were braced by 2 in. × 4 in. blocking in between and mounted on two layers of 1.3 cm (½ in.) plywood.

The aluminum flashing termite shield was placed on the knee wall. The first layer of straw was placed in position and covered by a plastic moisture barrier. Subsequent rows of bales were added, as shown in Figure 7. As bales were added, connection pins and staples were placed as indicated in Figure 8. Air spaces created between bales were filled with loose straw. The 21 bales chosen for the test wall and their location within the test wall are shown in Figure 9. Twenty-four stakes were driven into the stacked bales, so that the flat end was flush with the surface of the bales on the drywall side, approximately 60.9 cm (24 in.) apart to serve as studs for the gypsum board. The tips of the stakes were cut off flush with the straw bale surface on the stucco side. Chicken wire 1.27 cm mesh (½ in.) was draped over the top of the wall to cover both sides and secured to the side bracing and knee wall. The top plate was constructed as shown in Figure 6 and placed on the top layer of straw bales in the test wall. Compression rods were inserted through pre-drilled holes in the top plate. Washers and nuts were placed on the compression rods to increase tension. The wall was compressed by 10.2 cm (4 in.). Stucco was applied to one side of the wall, as shown in Figure 10, varying in thickness from 1.3 cm to 4.8 cm (½ in. to 2 in.). Two layers of 1.3 cm (½ in.) gypsum board were attached to the other side. Twenty-nine thermocouples were attached to each side of the wall, positioned as shown in Figure 11.

The newly constructed straw-bale wall was allowed to cure in the laboratory for 30 days and then placed in the hot box (shown in Figure 12) and tested in accordance with ASTM C 236-89 (Kosny et al. 1997). The metering chamber was kept at 38°C (100°F) and the climate chamber at 10°C (50°F). The mean test wall temperature was 24°C (75°F).

HOT BOX EXPERIMENTAL RESULTS

The data collected from the straw-bale clear wall experiment were evaluated using the procedures specified in the *Standard Test Method for Steady-State Thermal Performance of Building Assemblies by Means of a Guarded Hot Box* (ASTM). The objective was to determine thermal performance for a wall made of straw bales as described in the procedure. Results of the calculations are provided in Table 2,

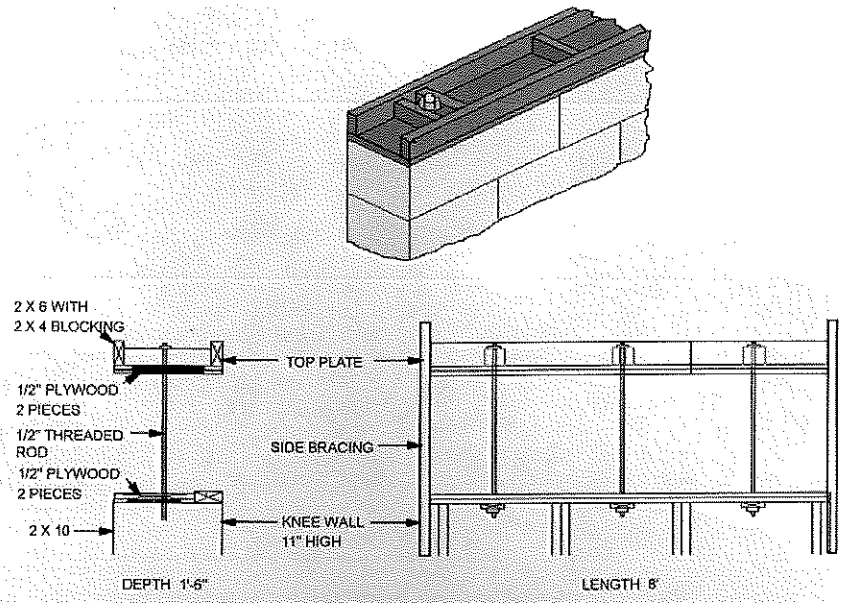

Figure 6 *Structural framework showing the knee wall and top plate.*

Figure 7 *Seven layers of bales made up the wall.*

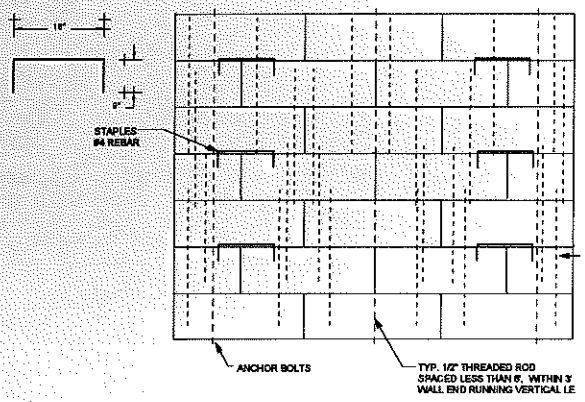

Figure 8 *Location of the compression rods, bale stables, and bale pins.*

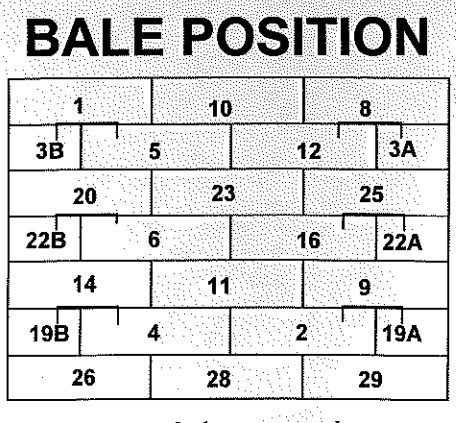

Figure 9 *Twenty-one bales were used to construct the test wall; bale properties are in Table 1.*

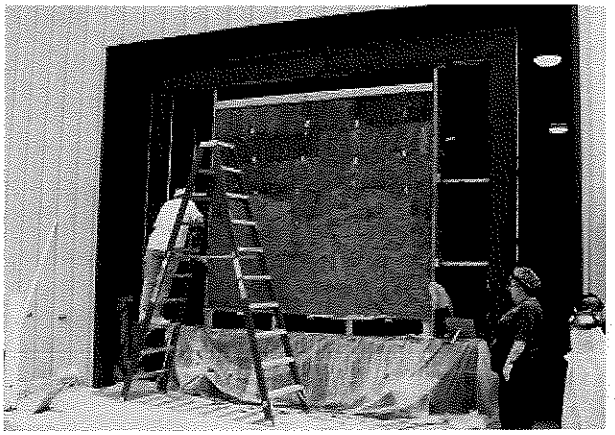

Figure 10 *Stucco was applied by hand on the exterior surface.*

Thermocouple Location

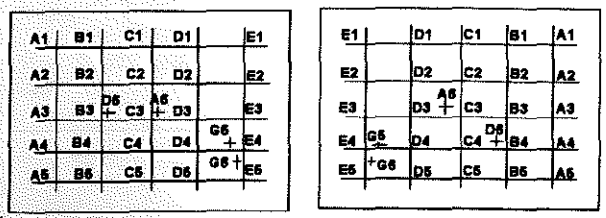

INTERIOR WALL **EXTERIOR WALL**

*A6 - 2X4 STAKE
*D6 - 2X4 STAKE
*G5 - 2X4 STAKE
*G6 - 2X4 STAKE

Figure 11 *Twenty-nine thermocouples were attached to each side of the test wall.*

DIAGRAM OF GUARDED HOT BOX

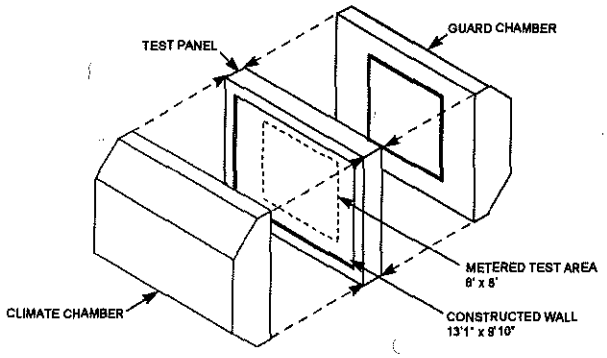

Figure 12 *Straw bale wall tested in ASTM C-236 guarded hot box.*

TABLE 2
Summary of Test Results Compiled on Straw-Bale Clear Wall

Variables	Sample Time 218.00 to 221.75 (I-P)	Sample Time 218.00 to 221.75 (SI)	Sample Time 220.00 to 225.75 (I-P)	Sample Time 220.00 to 225.75 (SI)
M-air (th) (°F/°C)	110.00	43.33	110.00	43.33
M-MPH MPH/KmPH	1.34	2.14	1.34	2.14
M-Straw (°F/°C)	108.20	42.33	108.11	42.28
M-Stake (°F/°C)	108.34	42.41	108.26	42.36
M-Staple (°F/°C)	108.38	42.43	108.27	42.37
M-Surface Area (°F/°C)	108.20	42.33	108.12	42.29
C-Air (°F/°C)	51.27	10.71	52.00	11.11
C-MPH/KmPH	1.42	2.27	1.26	2.02
C-Straw (°F/°C)	52.96	11.64	52.81	11.56
C-Stake (°F/°C)	52.69	11.50	52.45	11.36
C-Staple (°F/°C)	53.00	11.67	52.66	11.48
C-Surface Ave. (°F/°C)	52.95	11.64	52.80	11.55
Panel Mean (°F/°C)	80.58	26.99	80.46	26.92
Thermopile Output Diff. (°F/°C)	–0.15	-0.08	–0.16	–0.09
M-Chamber Q (Btu/h/W)	222.62	65.24	230.41	67.53
R-Value (s-s) $h \cdot ft^2 \cdot °F/Btu$ ($m^2 \cdot K/W$)	15.88	2.80	15.37	2.71
Ru-Value $h \cdot ft^2 \cdot °F/Btu$ ($m^2 \cdot K/W$)	16.88	2.97	16.11	2.84
Rms Value $h \cdot ft^2 \cdot °F/Btu$ ($m^2 \cdot K/W$)	0.52	0.09	0.52	0.09
Rcs-Value $h \cdot ft^2 \cdot °F/Btu$ ($m^2 \cdot K/W$)	0.48	0.09	0.22	0.04

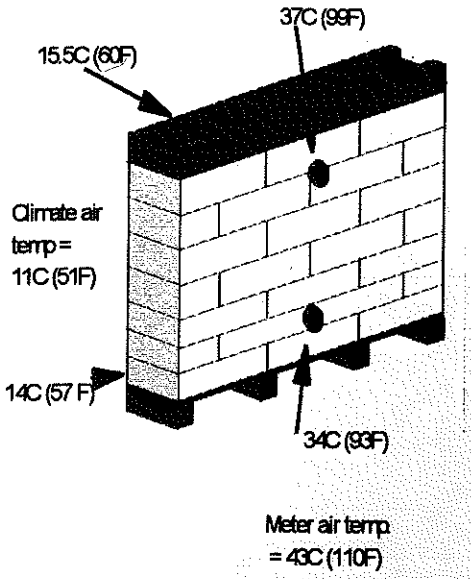

Figure 13 This isometric drawing of the straw bale test wall shows the location of the thermocouple placement that measured lateral temperature gradients between the straw and facings.

which has four R-values representing thermal resistance of the constructed wall. They are: R-value (s-s): surface-to-surface thermal resistance; Ru-value: air-to-air thermal resistance, which includes air film resistances; Rms-value: air film resistance on meter side of wall; Rcs-value: air film resistance on climate side of wall. Two consecutive four-hour periods were selected for analysis based on the criteria specified in ASTM C 236-89, sections 8.2.1 and 8.2.2. During these time periods, climate-side thermal variance was minimal.

The thermal resistance (R-Value) is calculated by

$$R = \frac{A(t_1 - t_2)}{(Q_h + Q_f)} \quad (1)$$

where

R = thermal resistance of wall assembly, $m^2 \cdot K/W$ ($h \cdot ft^2 \cdot °F/Btu$);

A = area of metering chamber, 5.3 m^2 (64 ft^2);

t_1 = average surface temperature of the wall assembly on the metering side, °C (°F);

t_2 = average surface temperature of the wall assembly on the climate side,° C (°F);

Q_h = metering heater energy input, W (Btu/h);

Q_f = metering fan energy input, W (Btu/h).

The overall thermal resistance (R-value) is calculated by

$$R_u = \frac{A(t_h - t_c)}{(Q_h + Q_f)} \quad (2)$$

where

R_u = overall thermal resistance of wall assembly, $m^2 \cdot K/W(h \cdot ft^2 \cdot °F/Btu)$;

A = area of metering chamber, 5.3 m^2 (64 ft^2);

t_h = average meter-side air temperature, °C (°F);

t_c = average climate-side air temperature, °C (°F);

Q_h = metering heater energy input, W (Btu/h);

Q_f = metering fan energy input, W (Btu/h).

The meter-side air film thermal resistance ($R_{ms\ air}$) is calculated by

$$R_{ms\ air} = \frac{A(t_h - t_1)}{(Q_h - Q_f)} \quad (3)$$

where

$R_{ms\ air}$ = meter-side air film thermal resistance, $m^2 \cdot K/W(h \cdot ft^2 \cdot °F/Btu)$;

A = area of metering chamber, 5.3 m^2 (64 ft^2);

t_h = average meter-side air temperature, °C (°F);

t_1 = average surface temperature of the wall assembly on the metering side, °C (°F);

Q_h = metering heater energy input, W (Btu/h);

Q_f = metering fan energy input, W (Btu/h).

The climate-side air film thermal resistance ($R_{cs\ air}$) is calculated by

$$R_{cs\ air} = \frac{A(t_2 - t_c)}{(Q_h + Q_f)} \quad (4)$$

where

$R_{cs\ air}$ = climate-side air film thermal resistance, $m^2 \cdot K/W$ ($h \cdot ft^2 \cdot °F/Btu$);

A = rea of metering chamber, 5.3 m^2 (64 ft^2);

t_2 = average surface temperature of the wall assembly on the climate side,°C (°F);

t_c = average climate-side air temperature, °C (°F);

Q_h = metering heater energy input, W (Btu/h);

Q_f = metering fan energy input, W (Btu/h).

Metering box wall losses were not included in any of the energy balance calculations. In the worst case, the metering box wall loss represents less than 0.2% of the energy input ($Q_h + Q_f$).

The thermal performance of the tested wall, given as an R-value, was in the range of 2.8 $m^2 \cdot K/W$ (16 $h \cdot ft^2 \cdot °F/Btu$) when literature searches suggested values in the range of 7 $m^2 \cdot K/W$ (40 $h \cdot ft^2 \cdot °F/Btu$). This discrepancy was a concern and possible explanations were considered. The first concern was the accuracy of the test result. The straw bale wall was removed and a calibrated panel of known resistance was installed and tested. The result was within 2% of the calibration panel known thermal resistance. The speculation that there was convection within the wall led to installation of four thermocouples positioned as shown in Figure 13 between the straw and drywall on the meter side (interior) and the straw and stucco on the climate

TABLE 3
Directional Properties of Straw Bales

Fiber Direction	Thermal Resistance (m·C/W)	Thermal Resistance (h·ft²·°F/Btu·in.)	Thermal Conductivity (W/m·K)	Airflow Permeability (10^{-9} m²)	Specimen Density (kg/m³)
Parallel	12.3	1.77	0.0815	110	62.3
Perpendicular	17.5	2.53	0.0570	63	81.0

side (exterior). While the test wall metering surface area temperature did not vary by more than .5°C, the 3°C (5.4°F) temperature gradient behind the drywall from the top to the bottom of the wall is a strong indication that this wall has the potential for internal natural convection.

MATERIAL PROPERTY MEASUREMENTS

Measurements of the straw's thermal conductivity and airflow permeability were made for straw obtained from the same stack used to construct the full-scale wall. Small samples of the straw were compressed into wooden boxes to a density similar to the average straw bales shown in Table 1 for the perpendicular test specimen but were less than the average density for the parallel specimen. One box contained the straw in such a manner that the conductivity and air permeability could be measured for heat and airflow parallel with the fiber direction, the other perpendicular to the fibers. The thermal conductivity measurements were made with the heat flow in the downward direction to prevent any possible convective effects. The straw material property characteristics measured are listed in Table 3.

The airflow permeability was measured in an apparatus built in the ORNL materials laboratory. The apparatus is based on Darcy's law, which states that the airflow rate is proportional to a material's permeability divided by the length of the airflow path. This rig was built to measure the airflow permeability of insulation materials such as cellulose, rock wool, and fiberglass (Wilkes and Graves 1993). For airflow perpendicular to the straw fibers, the permeability was 63×10^{-9} m². For airflow parallel to the fibers, the permeability was 110×10^{-9} m². For comparison, the permeability of low-density loose-fill fiberglass attic insulation (which was shown to convect in the ORNL Large Scale Climate Simulator and which led to usage restrictions in Minnesota) was 60 to 80×10^{-9} m² (Wilkes and Graves 1993). So airflows in parallel with the straw fibers average 60% greater than those found in the most common commercial insulation with the highest documented airflow permeability.

Simplified Prediction of Convection Based on Material Property Measurements

The airflow permeability of straw can be used to determine the potential effect of convective heat transfer within the straw. The Rayleigh number, a ratio of the effects of buoyancy, viscous drag, and thermal diffusivity, is used with empirical correlations to determine the effect of convection within a porous media.

$$Ra = \frac{c_\rho \rho^2 g K L \beta \Delta T}{\mu \lambda} \quad (5)$$

where

Ra = Rayleigh number,
c_ρ = specific heat of air,
ρ = density of air,
g = gravitational acceleration,
L = wall thickness,
β = volumetric expansion coefficient of air,
ΔT = temperature difference,
μ = dynamic viscosity of air, and
λ = thermal conductivity of the porous medium.

Within a porous media, the length scale in the Rayleigh number is provided by the measured permeability and the thickness of the material. For a vertical wall with horizontal heat transfer, the height of the wall is used instead of the thickness of the wall (Bejan 1995; Nield and Bejan 1992). The thermal conductivity is that of the porous material measured under conditions without convection.

Empirical and analytical work on vertical porous structures heated from one side found that when the square root of the Raleigh number is greater than the ratio of wall height to width, convection can occur (Bejan 1995; Nield and Bejan 1992). The straw bale test wall height to thickness ratio equals 5.3, using 2.4 m height and 46 cm thickness (8 ft height and 18 in. thickness). The Rayleigh number for the straw bale test wall is 119, using (1) the thermal conductivity parallel to the fibers (because that is the direction of the conductive heat transfer), (2) the permeance perpendicular to the fibers (because that represents the chief impediment to convective heat transfer), (3) a mean temperature of 298 K (77.5°F), and (4) a temperature difference of 25 K (45.4°F)—the wall thickness is derived by height, not width. The resulting square root of the Raleigh number is 11; thus, some convection would be expected. Equation 6 is an empirical correlation developed for the prediction of the heat transfer due to convection in a homogeneous porous medium such as the straw bale test wall under steady-state conditions with constant temperatures on both sides (Bejan 1995).

$$\frac{Q_{total}}{Q_{conduction}} = 0.508\frac{L}{H}\sqrt{Ra_H} \quad (6)$$

where

Q_{total} = total heat flux,

$Q_{conduction}$ = conductive heat flux,

H = wall height, and

Ra_H = Rayleigh number based on height.

Bejan's equation predicts that internal convection within the straw bale test wall would decrease the predicted R-value based only on conduction by less than 5%. However, as shown by the hot box test results in Table 2, the R-value for the 47 cm (18 in.) wall was 2.8 $m^2 \cdot K/W$ (16 $h \cdot ft^2 \cdot °F/Btu$). This value can be compared to the ASTM C 518 test results of the straw with parallel heat flow of 12.3 $m \cdot °C/W$ (1.77 $h \cdot ft^2 \cdot °F/Btu \cdot in.$) from Table 3, which gives a total resistance of 5.6 $m^2 \cdot K/W$ (32 $h \cdot ft^2 \cdot °F/Btu$) for a 44 cm (18 in.) wall. The whole wall straw bale test results show almost twice the amount of heat transfer as expected from simple conduction through the straw. Why?

BACK TO CONDUCTION

If not convection, then what about thermal shorts caused by some of the other materials used to construct the wall? Another conductive heat flow path considered included the wood stakes that were used to anchor the drywall to the wall. The wood offers a thermal resistance of about 8.3 $m \cdot °C/W$ (1.2 $h \cdot ft^2 \cdot °F/Btu \cdot in.$) compared to the straw at 12.5 $m \cdot °C/W$ (1.8 $h \cdot ft^2 \cdot °F/Btu \cdot in.$). However, on an area-weighted basis, 24 two-by-four stakes only represent 1.5% of the 5.9 m^2 (64 ft^2) of tested clear wall area, a very small portion of the overall parallel/series heat conduction path.

What about all the metal that is buried in this wall? The largest contribution comes from the No. 4 steel reinforcing bar connection pins (twenty-four 1.3 cm [½ in.] diameter, 76 cm [30 in.] long), "all thread" steel compression rods (three 1.3 cm [½ in.] diameter, 2.6 m [8.5 ft] long), and the bale staples (there are six 61 cm [24 in.] long, 1.3 cm [½ in.] diameter, 76 cm [30 in.] long) also made from No. 4 steel reinforcing bar. All of this steel is embedded in the middle of the wall and runs perpendicular to the predominate heat flow path. The amount is about the same on a per weight basis as cold-formed light-gauge steel-frame wall systems, which are gaining some interest in residential construction around the world.

A three-dimensional finite difference computer simulation was run on the impact of a compression rod connected to the bottom plate. Since the end of the rod did extend beyond the metering area, this presented the largest potential contribution to a flanking loss. However, since the ends of these rods were surrounded with at least 23 cm (9 in.) of fiberglass insulation, the impact of this thermal short was also found to be minimal. The chicken wire did cross over the top of the wall and the metal sheathing used as a termite shield and hygroscopic break between the straw and the moist ground in a real application did run parallel to the heat flow through the test wall. Once again, on a net area percentage basis, even with the large conductivity of steel compared to straw, these materials did not contribute a measurable impact on the overall thermal performance of the wall. Thermocouples were placed on both surfaces of the wall at the locations of all the imbedded steel, and at all temperature measurement locations no significant deviation of surface temperature was detected from that of the other temperatures measured at locations of continuous straw cross sections.

Well, What About Moisture?

The bale moisture prior to stuccoing was around 11% by weight. After the wall was dismantled, each bale was once again measured for moisture content using the same moisture probe and it was found that all were below 10% by weight. The wall was allowed to cure for 30 days in the laboratory and tested in the hot box with about 38°C (100°F) on the meter side and 10°C (50°F) on the climate side for more than three weeks. There was no detectable drying in the last two weeks of the measurement period. Because the moisture was not excessive, it was felt that the average content throughout the testing period was representative of field conditions in relatively dry climates.

The "Gaps"

A computational fluid dynamics (CFD) model was developed to explore the potential for convection in the straw bale test wall. The wall model was a two-dimensional rectangle, 2.4 m high and 46 cm thick (8 ft high and 18 in. thick) with 1.27 cm thick gypsum on one side and 1.27 cm stucco on the other. The gypsum side of the rectangle was given a convective boundary condition with an ambient temperature of 310.9 K (100°F) and a convective heat transfer coefficient of 8.29 $W/m^2 \cdot K$ (2.6 $Btu/h \cdot ft^2 \cdot °F$). The gypsum had a thermal conductivity of 0.16 $W/m^2 \cdot K$ (0.09 $Btu/h \cdot ft^2 \cdot °F$). The stucco side was given a similar convective boundary condition, with an ambient temperature of 285.7 K (55°F) and a convective heat transfer coefficient of 34.1 $W/m^2 \cdot K$ (10.8 $Btu/h \cdot ft^2 \cdot °F$). The stucco thermal conductivity was 0.106 $W/m^2 \cdot K$ (0.06 $Btu/h \cdot ft^2 \cdot °F$). The top and bottom were considered to be adiabatic. These ambient temperatures were chosen to be consistent with the hot box experimental conditions.

The model did not include the wooden stakes, steel compression rods, steel bale staples, chicken wire, aluminum termite shield, nor the steel connection pins for the reasons stated earlier in this paper. The model did include the directional values for airflow permeability within the straw but used a single isotropic value for thermal conductivity within the straw and the air gap of 0.0815 $W/m \cdot °C$ (0.05 $Btu/h \cdot ft \cdot °F$). This is the same conductivity as measured using the straw specimen with heat flow parallel to the fibers.

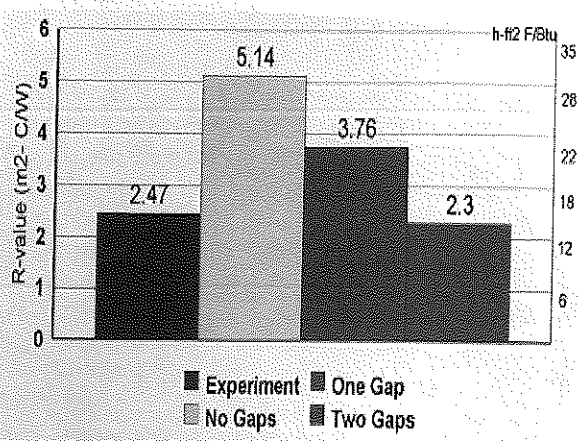

Figure 14 *CFD model results compared to hot box experiment.*

The resulting R-value predictions from this CFD parametric evaluation are summarized in Figure 14. The first model was to assume there were no gaps between the straw and the surface treatments. This led to an effective R-value prediction of 5.14 m·°C/W (29.2 h·ft^2·°F/Btu). This result includes both the conductive and convective heat transfer. About 17% of the resulting heat flow across this wall was due to internal natural convection. The hot box results for these same boundary conditions were an R-value of 2.47 m·°C/W (14 h·ft^2·°F/Btu). This illustrated that the convective short circuiting cannot all occur within the straw itself. This also suggests that if any such gaps could be eliminated, the expected R-value should be around 5 m·°C/W (30 h·ft^2·°F/Btu).

As suggested earlier, the temperature gradient found between the straw and the surface treatments suggested convection just behind the drywall and stucco layer. When the wall was dismantled, particular attention was given to this region. Irregular gaps were found and carefully examined. The gap on the drywall side of the wall was a 1.3 cm to 2.6 cm (½ in. to 1 in.) thick covering approximately 60% of the wall face. The gap on the stucco (climate) side was an uneven space, 0.3 cm to 0.6 cm (1/8 in. to ¼ in.) thick, covering approximately 20% of the wall face. The nonuniform air gaps were modeled as 1.9 cm (0.75 in.) thick space between the gypsum and the straw and a 0.64 cm (0.25 in.) thick space between the stucco and the straw. The airflow permeability of these irregular porous spaces is the major unknown.

This uncertainty was addressed by parametrically varying the airflow permeance (Stovall et al. 1997). The air gap behind the drywall was the most obvious passage for air movement; therefore, the model was first modified to reflect this gap with a permeance 100 times greater than used for air permeance through the straw, 11000 × 10^{-9} m^2 parallel to the fibers and 6290 × 10^{-9} m^2 perpendicular to the fibers. Opening up this one gap resulted in a decrease in predicted R-value to 3.76 m^2·°C/W (21.4 h·ft^2·°F/Btu), still higher than that found experimentally. From here the second gap under the

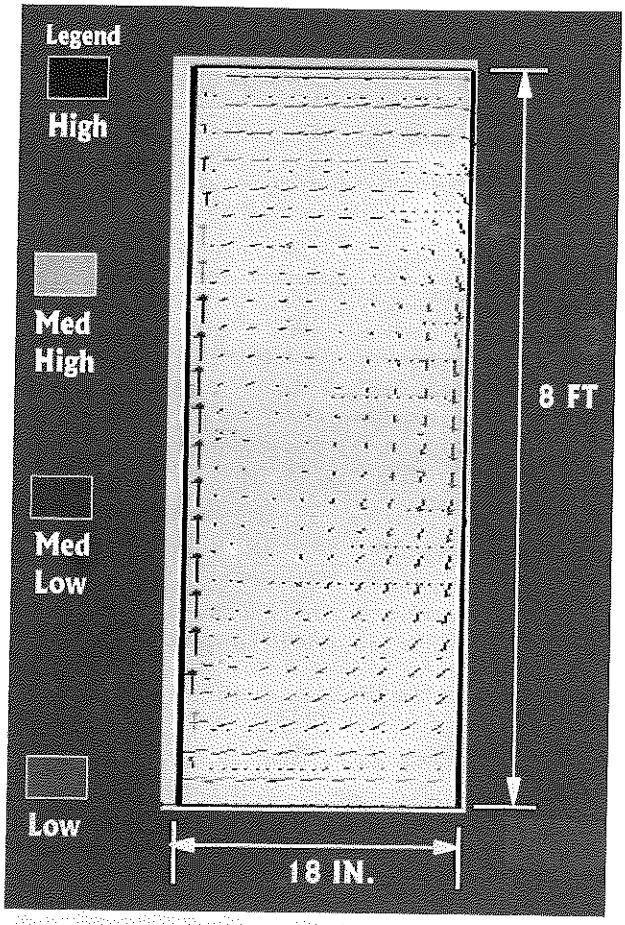

Figure 15 *Straw bale wall convective airflow pattern.*

stucco was added to the model by using permeance values, reduced from those used in the drywall gap proportionally to the ratio of gap widths between the drywall and stucco gap, 3300 × 10^{-9} m^2 parallel to the fibers and 1890 × 10^{-9}m^2 perpendicular to the fibers. The addition of this second gap led to a further drop in the predicted R-value to 2.3 m^2·°C/W (13 h·ft^2·°F/Btu). This was felt to be reasonably close to the whole wall experimental measurements. Therefore, the CFD modeling has confirmed that natural convection within the wall gaps could be responsible for the relatively low R-value measured in the full wall system test, compared to R-value predictions based on material property measurements.

Figure 15 shows a cross section of the straw bale wall with airflow arrows within the wall generated by the CFD modeling, which illustrates the strongest currents are on the left side of the rectangular wall model just behind the drywall. An examination of a possible design modification involving the introduction of horizontal airflow barriers, called *turbulaters*, was also made. These were relatively ineffective because alternative flow patterns developed that were equally effective in transporting heat though the wall. The R-value gains were negligible.

Based on the CFD modeling results and the evidence gained by the temperature gradient measurements in the loca-

tion of the gaps while the whole wall was under going the C-236 test, as shown in Figure 13, it is confirmed that there was significant heat transfer through convection currents within gaps formed between the straw and the surface treatments.

SUMMARY AND CONCLUSIONS

The first hot box test of a structural straw bale wall system resulted in about a 50% lower R-value, 2.8 $m^2 \cdot °C/W$ (16 $h \cdot ft^2 \cdot °F/Btu$), than is calculated from measured material thermal conductivity and airflow permeability properties of the anisotropic behavior of the straw alone. The data analysis and computational fluid dynamic computer modeling confirm that internal natural convection is a very likely cause for this discrepancy. However, only 5% to 17% of the convection occurs within the straw itself; instead, most of the convection actually occurs in the discontinuous gaps between the drywall and the straw bales and the stucco and the straw bales passing through the top and bottom row of bales.

Flat interior sheathing surface treatment certainly is an option, and for many applications it is necessary to have very smooth flat walls to meet housing market demands. However, plastering on the inside is generally the preferred finish in most of the new straw bale buildings being built today. In those buildings where drywall or sheet paneling is used, an effort should be made to fill the void between the bales and the back of the sheathing with a material of similar or lower permeability to straw bales. Obviously, careful bale stacking can minimize surface elevation changes in the wall, but one of the benefits of straw bale construction is the larger construction tolerances. The exterior test wall stucco was hand applied by an inexperienced stuccoing crew; however, professional stuccoing is expensive. The other option, of course, is to apply the stucco with a pumper truck. The air pressure used to transport the cementitious material onto the wall will tend to penetrate the straw better and minimize air gaps. Once again, applying stucco in this manner is expensive.

The straw bale test wall was built largely by hand, using a very low-skilled crew. For low- income housing, this could be a most sustainable construction practice. However, the construction is labor intensive and the use of steel rebar for stabilization stakes should be changed to a less energy intensive material, such as wood. The final product was a good quality wall and structurally very adequate. The authors feel this was a representative straw-bale wall with a recommended technique for adhering sheathing to one side. The authors recommended that a second wall be built with straw bale advocates and with stucco on both sides applied in a manner that minimizes air gaps. This wall was constructed and displayed on the Internet by transmitting digital photographs every minute for the two days of construction in February 1998. At the time this paper was written, the wall had been tested and the data displayed on the Internet (http://www.ornl.gov/roofs+walls/) for students to compute the R-value for themselves and as part of an Internet curriculum developed for the U.S. Department of Education.

ACKNOWLEDGMENTS

Special acknowledgment is given for the participation of the Appalachian Regional Commission Teacher Leadership Participants: Joseph Boutwell, Donna Boutwell, Judith Moody, Alma Greer, Brenda McMillan, Martha Cameron, Stewart Colley, Ronald Newell, Dennis Deel, Charles Sturgil, Deborah Ruggles, Melody Troy, Carrie Stewart, Janis Wood, Roger Spry, Ronnie Cashen, Darrell Silcox, and Luther Taylor.

Research for this test was sponsored by the Office of Buildings Technology and Community Systems, U.S. Department of Energy.

REFERENCES

ASTM. 1989. *ASTM C 236-89, Standard test method for steady-state thermal performance of building assemblies by means of guarded hot box.* ASTM Standards, Vol. 04.06, pp. 53-63. American Society for Testing and Materials.

Bejan, A. 1995. *Convection heat transfer*, 2d ed. New York: John Wiley & Sons, Inc.

CMHC. 1984. An innovative straw-bale/mortar wall system. NHA 5799 84/08. CMCH Housing Technology Incentives Program, Canadian Housing Information Centre, Canada Housing and Mortgage Corp.

Fluent, Inc. 1993. *Fluent user's manual.* Lebanon, N.H.: Fluent, Inc.

Huang, J. 1995. House of straw. U.S. Department of Energy and Renewable Energy, DOE/GO 10094-01, April.

Kosny, J., A. Desjarlais, and J. Christian. 1997. Whole wall rating/label for metal stud wall systems with sprayed polyurethane foam; Steady state thermal analysis. Oak Ridge National Laboratory, June.

MacDonald, S.O., and M. Myhrman. 1995. *Build it with bales: A step by step guide to straw bale construction*, Version 1.0.

McCabe, J. 1993. The thermal resistivity of straw bales for construction (e-mail: energyi@dcez.com) (URL: <http://solstice.crest.org/efficiency/straw_insulation/results.html>).

Nield, D.A., and A. Bejan. 1992. *Convection in porous media.* New York: Springer-Verlag.

Stovall, T.K., K.E. Wilkes, J.E. Christian, F.J. Weaver, and G.E. Nelson. 1997. A review of Oak Ridge National Laboratory's research addressing potential sustainable insulation materials. Presented at the Building Environment and Thermal Envelope Coordinating Council of the National Institute of Building Science on Sustainable Materials, November.

Wilkes, K.E., and R.S. Graves. 1993. Air-flow permeability of attic insulation materials. ORNL/M-2646, Oak Ridge National Laboratory, September.